December 2010 ISSN : 0974 - 7486 Volume 6 Issue 4

Trade Science Inc.

Materials Science

An Indian Journal

Full Paper

MSAIJ, 6(4), 2010 [260-266]

As-Cast microstructures of {M-30Cr-0 to 5% C} ternary alloys. Part 1: Nickel-Base alloys

Patrice Berthod[1,2]*, Elise Souaillat[1], Ophélie Hestin[1]

[1]Faculty of Sciences and Technologies, B.P. 70239, 54506 Vandoeuvre-les-Nancy, (France)

[2]Institut Jean Lamour (UMR 7198), Department of Chemistry and Physics of Solids and Surfaces, B.P. 70239, 54506 Vandoeuvre-les-Nancy, (France)

E-mail : Patrice.Berthod@lcsm.uhp-nancy.fr

Received: 29th July, 2010 ; Accepted: 8th August, 2010

ABSTRACT

High carbides fractions can be easily obtained in alloys, simply by choosing sufficiently high carbon contents in presence of a carbide-former metallic element. In this study, nickel alloys containing simultaneously high contents in carbon and chromium were preliminary studied by thermodynamic calculations, then elaborated by foundry. Their microstructures were observed by electron microscopy. The Ni-30Cr alloys with less than 2wt. %C display a hypoeutectic microstructure composed of matrix dendrites and eutectic M_7C_3 carbides. For carbon contents higher than 2-2.5 wt. %, coarse carbides have replaced the dendrites, and the double carbides population, eutectic and pro-eutectic, can be of two natures: M_7C_3 and M_3C_2. If more than 4wt.% C is present, graphite appears and the increase in carbides with carbon is limited.

KEYWORDS

Nickel alloys;
High chromium;
Very high carbon;
Thermodynamic calculations;
Solidification;
Microstructure.

INTRODUCTION

Cast nickel base alloys are widely used for numerous applications, and notably their chromium–rich versions can be met in several domains, in dentistry (e.g. prostheses' reinforcing frameworks)[1,2] or in aeronautics (notably turbine blades[3,4]) for instance, for which chromium brings the alloys a good resistance against either aqueous corrosion or high temperature oxidation.

Carbon can be added to such {Ni, Cr}–based alloys in order to obtain more or less high levels of mechanical resistance, and particularly of hardness[5-8] thanks to the high values of this property shown by carbides[9]. Indeed, carbides easily precipitate during solidification, which can result in a double-phased alloy with a ductile metallic phase (FCC nickel matrix, hardness of only about one hundred Vickers) and a hard carbide phase which can be $Cr_{23}C_6$ (1650 Hv_{50g}), Cr_7C_3 (1336 Hv_{50g}) or Cr_3C_2 (1350 Hv_{50g})[9]. Since the hardness of the whole alloy logically increases in nickel-based alloys with the carbides volume fraction[10] (which itself increases with the carbon content[11]), it is interesting to know the carbides quantities which can be obtained by increasing the mass of carbon added to the alloy in presence of a carbide-former element.

This is the aim of this work in which a wide variety of nickel-based alloys containing a high amount of chromium, which plays here the role of the carbide-former element, has been elaborated by foundry, after one has simulated the probable microstructures using thermodynamic calculations, in order to observe the evolution of the quantity of carbides from the absence of carbon up to very high carbon contents (at the level of hypereutectic cast irons).

EXPERIMENTAL

Preliminary thermodynamic calculations

Before any real elaboration of alloys thermodynamic calculations may give useful indications about the microstructures which can be expected, notably concerning the type and the quantities of carbides, as well as the possible appearance of other phases as intermetallic ones, graphite (in the case of the highest carbon contents), ... Such calculations were performed using the N-version of the Thermo-Calc software[12] and a database containing the descriptions of the Ni-Cr, Ni-C, Cr-C and Ni-Cr-C systems[13-15]. The microstructures at the thermodynamic stable states were thus calculated at 1500°C, 1400, 1300, ... down to 0°C, the latter results being of course not realist, but allowing to see what would be obtained theoretically if diffusion and transformations were still possible at ambient temperature.

Elaboration and metallographic characterization of the alloys

The targeted carbon contents in the thirteen Ni-30wt. %Cr-xC alloys were 0 (alloy named "Ni00"), 0.2 (Ni02), 0.4 (Ni04), 0.8 (Ni08), 1.2 (Ni12), 1.6 (Ni16), 2.0 (Ni20), 2.5 (Ni25), 3.0 (Ni30), 3.5 (Ni35), 4.0 (Ni40), 4.5 (Ni45) and 5.0 wt. %C (Ni50). All the alloys were elaborated by foundry from pure elements (nickel and chromium: Alfa Aesar, purity higher than 99.9 wt.%; carbon: graphite), and an ingot of several tens grams was obtained for each alloy. In each case, nickel, chromium and graphite were melted together, under an inert atmosphere of 300 mbars of Argon U, in the water–cooled copper crucible of a CELES high frequency induction furnace. Fusion, as well as solidification, was achieved in the copper crucible. Each ingot was cut, embedded in a resin + hardener mixture (Escil CY230 + HY956), and polished with SiC paper from 240 to 1,200 grit and finished using a 1µm diamond–paste.

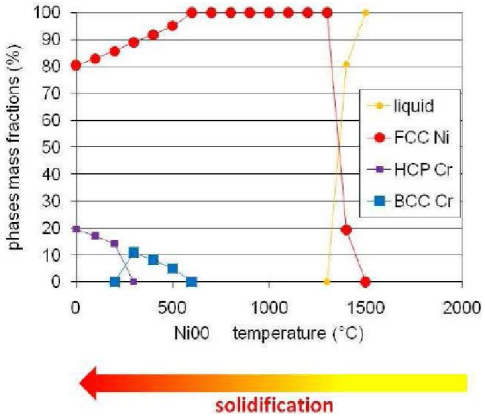

Figure 1 : Stable metallurgical states of the Ni00 alloy as calculated by Thermo-Calc; qualitative illustration of the microstructures development during the solidification progress

The mounted samples were metallographically characterized using a Scanning Electron Microscope (SEM: Philips, model XL30), essentially in Back Scattered Electrons mode (BSE, 20kV). Several images were taken at the magnification ×500 or ×1000 and used to estimate the carbides surface fractions (and of graphite when present) by image analysis (software Adobe Photoshop CS).

RESULTS AND DISCUSSION

Thermodynamic calculations

The theoretic microstructures of the Ni00 alloy (Ni-30Cr) at 1500°C, 1400°C, ... calculated using Thermo-Calc are represented by the graph given in figure 1, which can be considered as a qualitative description of the solidification sequences, at least when temperature is high enough to allow the phase transformations to be not too far from the successive thermodynamic equilibria corresponding to the decreasing temperature. At very high temperature the liquid phase is replaced by the austenitic Face Centred Cubic matrix which remains alone until reaching about 500°C. The alloy remains then not longer single-phased since a part of matrix obviously transforms into a Body Centred Cubic

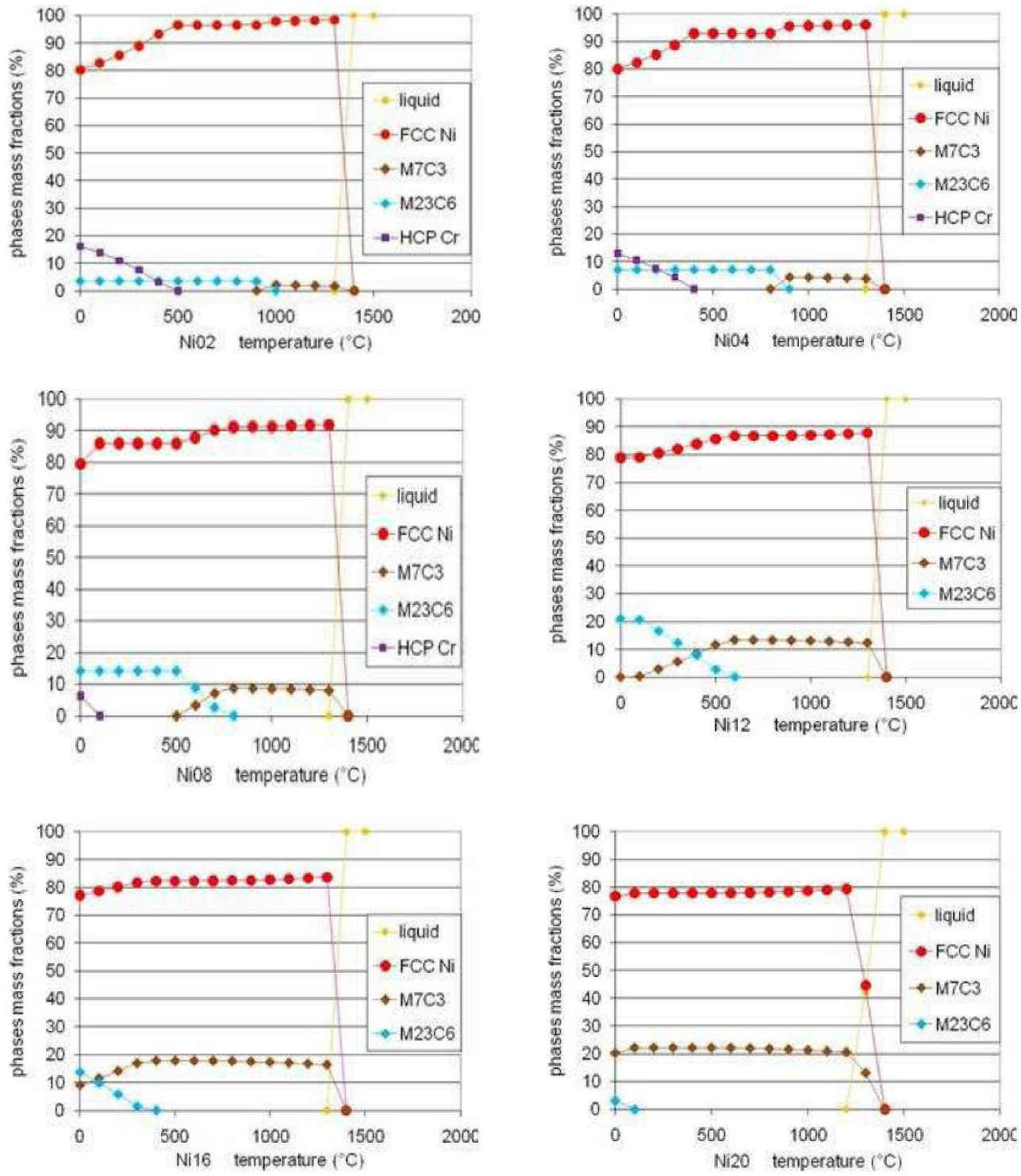

Figure 2 : Stable metallurgical states of the Ni02 to Ni20 alloys as calculated by Thermo-Calc; qualitative illustration of the microstructures development during the solidification progress

allotropic crystalline network, before that a Hexagonal Compact Phase rich in chromium (more than 99.9wt. %Cr) appears.

The presence of carbon induces the appearance of carbides. In the Ni02 alloy (Figure 2), the dendritic FCC nickel matrix forms first, while eutectic M_7C_3 carbides precipitate at a lower temperature (about 2% in mass). During the cooling they disappear near 1000°C because the replacement of these high temperature carbides by the low temperature ones $M_{23}C_6$ (about 3.5% in mass).

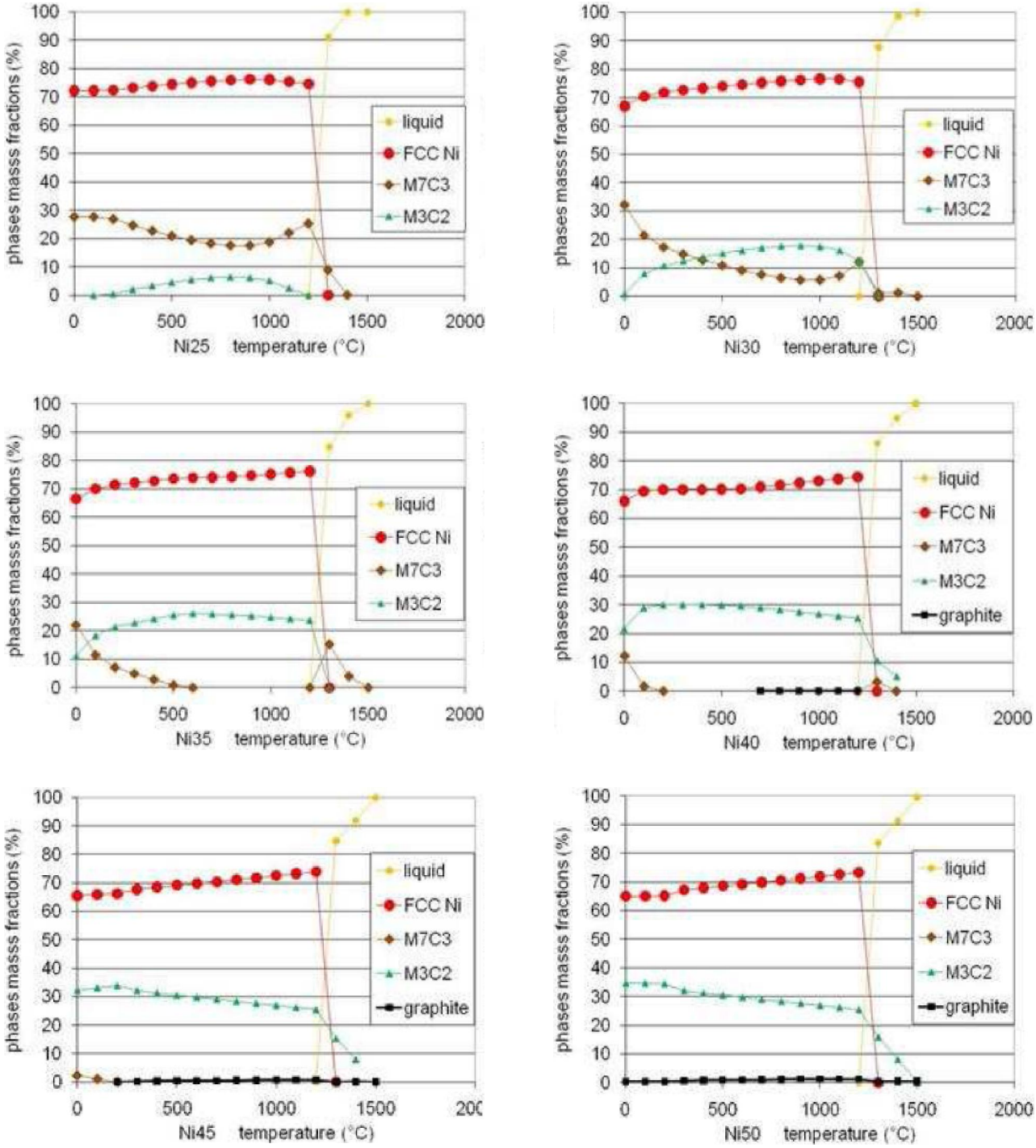

Figure 3 : Stable metallurgical states of the Ni25 to Ni50 alloys as calculated by Thermo-Calc; qualitative illustration of the microstructures development during the solidification progress

Near 500°C again, a part of the FCC matrix is replaced by the HCP network, more and more during the cooling down to room temperature.

The same features are observed for Ni04 (4.3 mass.% M_7C_3 then 7 mass % $M_{23}C_6$), Ni08 (8.5 mass % M_7C_3 then 14 mass % $M_{23}C_6$) and Ni12 (13 mass % M_7C_3 then up to 20 mass % $M_{23}C_6$) and Ni16 (17.5 mass.% M_7C_3 then up to 13 mass.% $M_{23}C_6$ with still 9% of remaining M_7C_3). In the Ni20 alloy, for which the solidification start is characterized by the simultaneous appearances of the matrix and of the M_7C_3 carbides (with even a short advance of the carbides), the M_7C_3

Full Paper

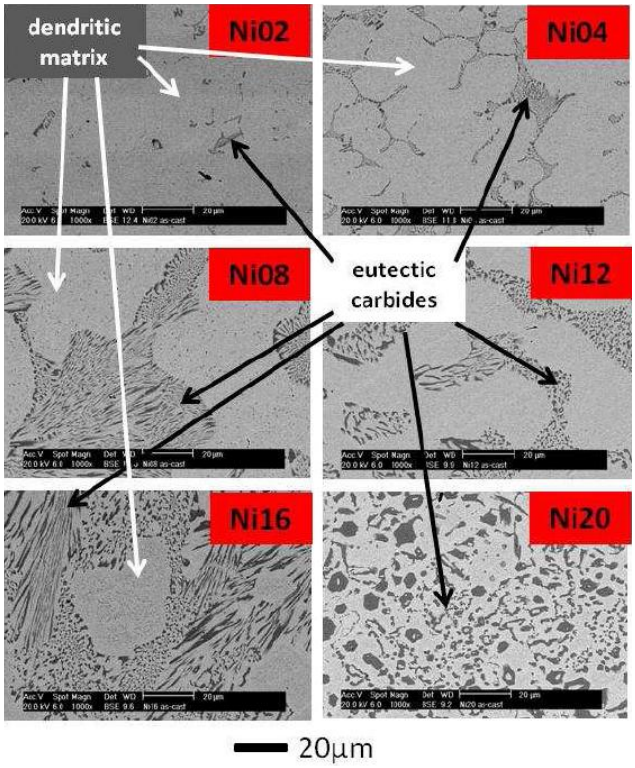

Figure 4 : As-cast microstructures of the Ni02 (hypoeutectic) to Ni20 (slightly hypereutectic) alloys

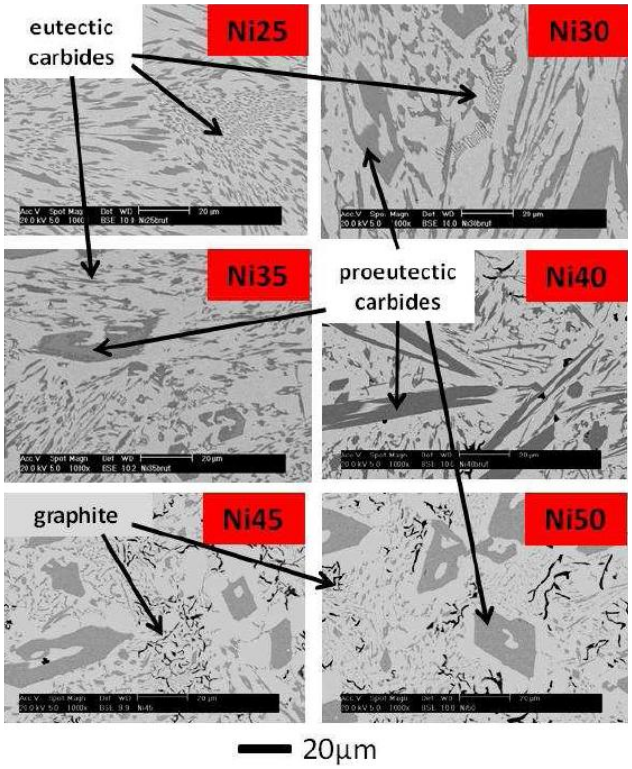

Figure 5 : As-cast microstructures of the Ni25 (hypereutectic) to Ni50 (very hypereutectic) alloys

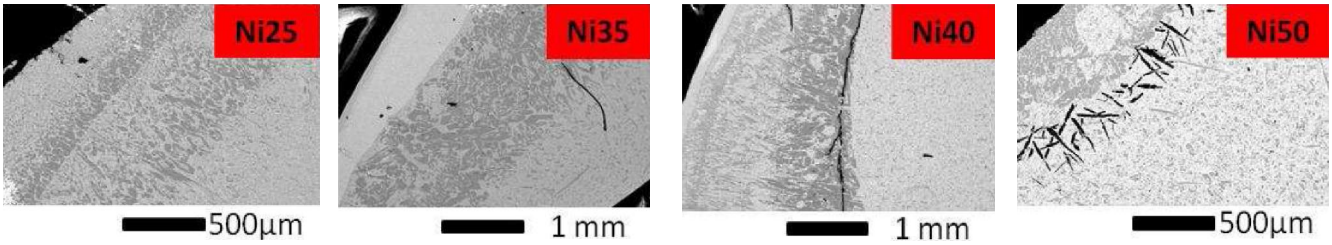

Figure 6 : Illustration of the microstructure heterogeneity {external part/ingot's center} probably resulting from movement of precipitated hypereutectic carbides during solidification

remain at about 22 mass percent of the alloy over the whole temperature range of solid state. From the Ni25 (even Ni20) alloy to the Ni35 alloy the first solid to appear is the M_7C_3 carbide (figure 3), with after around 25 to 28 mass % of carbides: M_7C_3 and M_3C_2 together (there is a more and more extended temperature range for the existence of M_3C_2 when the carbon content increases). For the Ni40, Ni45 and Ni50 alloys, the M_3C_2 has become the main then the unique carbide present with respectively 25-30, 25-33 and 25-34 mass % of carbides. For the same alloys the graphite phase appears, first in the solid state just after the solidification's end (Ni40) but as the first solid to appear in the case of the Ni45 and Ni50 alloys. However graphite disappears thereafter at a temperature which decreases when the alloy carbon content increases.

As-cast microstructures of the elaborated alloys

Figure 4 displays the microstructures of the Ni02 to Ni20 alloys in the as-cast condition, while the ones of the Ni25 to Ni50 alloys are illustrated in figure 5. Globally the previous calculation results are consistent with the observed microstructures in the centres of the ingots. The surface fraction of carbides effectively (and logically) increases with the carbon content in the alloy, and there is often a good correspondence between the fraction of the different phases (carbides or graphite) between thermodynamic calculations and results of image analysis. The latter were performed, with Photoshop, generally for pictures taken at ×500 or

×1000, and the surface fractions, assumed to be close to the volume fractions, were converted in mass fractions using 6.86 g/cm^3 for carbides (average of the densities of all types of carbides: 6.97 ($M_{23}C_6$), 6.92 (M_7C_3), 6.68 (M_3C_2) g/cm^3 [9]), 8.12 g/cm^3 for matrix and 2.25 g/cm^3 for graphite.

The comparisons between the as-cast phase fractions and the predicted ones which can be done are the following:

Ni02 alloy: 1.9 surf. % of carbides, as is to say 1.6 mass.% (to compare to 1.6 – 3.5 mass.% calculated depending on temperature),

- Ni04 alloy: 5.0 surf. % of carbides, i.e. 4.2 mass. % (to compare to 3.8* –7.4** mass. % calculated)
- Ni08 alloy: 12.2 surf. % of carbides, i.e. 10.5 mass. % (to compare to 8.1 –14.1 mass. % calculated)
- Ni12 alloy: 13.6 surf. % of carbides, i.e. 11.7 mass. % (to compare to 12.3 –21.1 mass. % calculated)
- Ni16 alloy: 18.3 surf. % of carbides, i.e. 15.9 mass. % (to compare to 16.4 –22.9 mass. % calculated)
- Ni20 alloy: 24.6 surf. % of carbides, i.e. 21.6 mass. % (to compare to 20.7 –23.3 mass. % calculated)
- Ni25 alloy: 25.6 surf. % of carbides, i.e. 22.5 mass. % (to compare to 25.4 –27.8 mass. % calculated)
- Ni30 alloy: 33.1 surf. % of carbides, i.e. 29.4 mass. % (to compare to 24.5 –33.0 mass. % calculated)
- Ni35 alloy: 31.9 surf. % of carbides and 0.11 surf. % graphite, i.e. 28.3 mass.% and 0.03 mass. % (to compare to respectively 23.8 –33.5 mass. % and 0% calculated)
- Ni40 alloy: 24.2 surf. % of carbides and 1.5 surf. % graphite, i.e. 21.4 mass. % and 0.44 mass. % (to compare to 25.4 –30.0 mass. % and max 0.19 mass. % calculated)
- Ni45 alloy: 27.0 surf. % of carbides and 3.3 surf. % graphite, i.e. 24.4 mass. % and 0.98 mass. % (to compare to 25.4 –33.7 mass. % and max 0.68 mass. % calculated)
- Ni50 alloy: 29.9 surf. % of carbides and 4.5 surf. % graphite, i.e. 27.4 mass.% and 1.35 mass.% (to compare to 25.5 –34.6 mass. % and max 1.2 mass. % calculated)

(* and ** for all alloys: * just after the solidification's end, ** at low/room temperature)

Concerning the carbides nature, the acicular morphology of the carbides contained by the present alloys with the lowest carbon contents in this study let think that they are effectively M_7C_3. In contrast there is seemingly a change of carbides nature in the alloys with the highest carbon contents, as displayed for example in the Ni35 alloy in which one can see in figure 5 coarse carbides with a double color when observed with the SEM in BSE mode: darker in its external part (probably M_3C_2) than in its internal part (probably M_7C_3), which would be here too in good agreement with calculations.

General commentaries

Over this wide interval of carbon contents one obtained a large variety of carbides fractions and also of different morphologies and natures of carbides. From the 0.2wt. %C to about 1.6-2wt. %C, carbides are only eutectic ones, and essentially M_7C_3. Even if they tend to transform into $M_{23}C_6$ at low temperature the high cooling rate (cooling in the copper crucible of the furnace) in the solid state did not really allow this nature change. For higher carbon contents, the composition of the alloy is obviously now on the other side of the eutectic valley, and solidification started, neither with the dendritic nickel matrix nor with the matrix-carbides eutectic compound, but with pro-eutectic carbides (M_7C_3, or M_3C_2 for the highest carbon contents) which are thereafter clearly visible in the microstructure: coarse elongated carbides, with a size which increases with the hypereutectic character of the alloy. For the very high carbon contents considered in this study, from 4 to 5 wt. %C (values which are at the level of hypereutectic cast irons), graphite appears, in conform to calculations. This light phase can also be the first solid to appear at the beginning of solidification, as the lamellar pro-eutectic graphite in grey cast irons.

If the hypo-eutectic alloys of this study were globally homogeneous in their microstructures, this was not the case of the hyper-eutectic alloys. Indeed, the external parts of the ingots were especially rich in carbides (Ni25 to Ni40 or 45) or both in carbides and coarse graphite (Ni50), as illustrated in figure 6. In contrast with the hypo-eutectic alloys for which solidification starts with the growth of austenitic dendrites of nickel solid solution with a good connection to one another, some of the pro-eutectic carbides or graphite, which are more independent and then free to move, were obviously driven outside of the liquid/mushy domain during the

pro-eutectic solidification. This type of segregation, which leads to a heterogeneous microstructure, was probably due to magnetic stirring or agitation generated by the induction heating. In some cases, the extremely high amount of the brittle carbide phase led to cracks (Ni40 in Figure 6), in addition to a probable extreme hardness. Image analysis led for example to 56 surf. % (52% in mass) of carbide in the external zone of Ni25, 53 surf. % (48 mass. %) in Ni30, 66 surf. % (62 mass. %) in Ni35, 64 surf. % (61 mass. %) in Ni40, 61 surf. % (57 mass. %) in Ni45 and 42 surf. % (41 mass. %) in Ni50 with also 8 surf. % (2.7 mass. %) of graphite.

CONCLUSIONS

Very high carbides fractions can be obtained in nickel chromium based alloys by adding great quantities of carbon, with as results probably very high levels of hardness and of wear resistance. For alloys too rich in carbon two phenomena can occur: precipitation of high quantities of pro-eutectic carbides which can lead to heterogeneity for the microstructure at the scale of the whole ingot, and appearance of carbides which limits the increase in carbides quantity (over a limit carbon content, new additional carbon induces the increase of graphite fraction and no more of carbide fraction). Obtaining higher fractions of carbides by increasing carbon over this limit, probably supposes higher contents in the carbide-former metal, here chromium.

ACKNOWLEDGEMENTS

The authors thank Lionel Aranda and Thierry Schweitzer for their technical assistance.

REFERENCES

[1] M.A.Engelman, C.Blechner; The New York Journal of Dentistry, **46**, 232 **(1976)**.
[2] E.F.Huget, N.Dvivedi, H.E.Cosner; The Journal of the American Dental Association, **94**, 87 **(1977)**.
[3] E.F.Bradley; 'Superalloys: A Technical Guide', ASM International, Metals Park, **(1988)**.
[4] C.T.Sims, W.C.Hagel; 'The Superalloys', John Wiley & Sons, New York, **(1972)**.
[5] A.Klimpel, L.A.Dobrzanski, A.Lisiecki, D.Janicki; Journal of Materials Processing Technology, **164-165**, 1068 **(2005)**.
[6] Z.T.Wang, H.H.Chen; Mocaxue Xuebao Tribology, **25**, 203 **(2005)**.
[7] H.Han, S.Baba, H.Kitagawa, S.A.Suilik, K.Hasezaki, T.Kato, K.Arakawa, Y.Noda; Vacuum, **78**, 27 **(2005)**.
[8] D.Zhang, X.Zhang; Surface and Coating Technology, **190**, 212 **(2005)**.
[9] G.V.Samsonov; 'Handbooks of High-Temperature Materials Properties Index', Plenum Press, New York, **2**, **(1964)**.
[10] P.Berthod, P.Lemoine, L.Aranda; Calphad, **32**, 485 **(2008)**.
[11] P.Berthod; Materials Science and Technology, **25(5)**, 657 **(2009)**.
[12] Thermo-Calc Version N: 'Foundation for Computational Thermodynamics', Stockholm, Sweden, Copyright **(1993, 2000)**.
[13] A.Dinsdale, T.Chart; MTDS NPL, Unpublished Work, **(1986)**.
[14] A.Gabriel, C.Chatillon, I.Ansara; High Temperature Science, **25**, 17 **(1988)**.
[15] J.O.Andersson; Calphad, **11**, 271 **(1987)**.